

Sum-weighted casein micelle AF4-UV-SAXS data disentangled - A new method for characterization and evaluation of widely size distributed samples

Hans Bolinsson^{a,1,*}, Martin Cramer Pedersen^{b,1}, Maria Glantz^a, Fátima Herranz-Trillo^c, Jacob Judas Kain Kirkensgaard^d, Lars Nilsson^a

^a Department of Process and Life Science Engineering, Faculty of Engineering LTH, Lund University, Lund, Sweden

^b Niels Bohr Institute, Faculty of Science, University of Copenhagen, Copenhagen, Denmark

^c MAX IV Laboratory, Lund University, Lund, Sweden

^d Department of Food Science and Niels Bohr Institute, Faculty of Science, University of Copenhagen, Copenhagen, Denmark

ARTICLE INFO

Keywords:

Casein micelles
SAXS
AF4
Evaluation
Sum-weighted data
Wide size-distribution

ABSTRACT

Casein micelles are key structures in milk, influencing stability, nutritional properties, and functionality. Their hierarchical architecture, which is dynamic and responsive to environmental conditions, plays a crucial role in dairy processing. Understanding the structural and dynamic properties of casein micelles is essential for optimizing dairy products and processing techniques. This study presents a novel method for characterizing and evaluating casein micelles using a combination of Asymmetrical Flow Field-Flow Fractionation (AF4) and Small-Angle X-ray Scattering (SAXS) at synchrotron facilities. By coupling AF4 with SAXS, we can fractionate milk samples according to micelle size and gain insights into their structural organization. However, the high-throughput data generated in such experiments pose challenges for traditional data analysis. We introduce an automated data processing pipeline utilizing the McSAS software in combination with Indirect Fourier Transformation, allowing for efficient fitting of SAXS data and extraction of structural parameters such as radius of gyration (R_g) and maximum particle dimension (D_{max}). This integrated approach provides a more detailed understanding of the heterogeneity and structural dynamics of casein micelles, revealing distinct features of their size distribution, internal cavities, and overall micelle structure across different fractions. The method offers a powerful tool for future investigations into the behavior of casein micelles under varying environmental conditions, with potential applications in optimizing dairy product formulations and studying casein micelle dynamics.

1. Introduction

Casein micelles are colloidal protein structures critical to the stability, nutritional properties, and functional behavior of milk. Consisting primarily of four different casein proteins, these micelles are stabilized by calcium phosphate clusters, forming a complex hierarchical architecture. This structure is highly dynamic and sensitive to environmental factors, such as pH, temperature, and ionic strength (Dalglish, 2011; Holt, 2022). Casein micelles play a central role in the industrial processing of milk, as their unique properties underpin a wide range of

dairy transformations. Understanding the detailed structure and dynamics of casein micelles is therefore essential for optimizing dairy processing techniques, such as ultrafiltration, heat treatment, renneting, and acidification, which in turn influence the texture, flavor, and stability of dairy products (Dalglish & Corredig, 2012; Tuinier & de Kruif, 2002). Moreover, the micelle's colloidal stability and reactivity are pivotal in developing innovative dairy-based functional foods, extending their relevance beyond traditional dairy products.

To gain a deeper insight into the structural organization of casein micelles, a combination of Small-Angle X-ray Scattering (SAXS) and

This article is part of a special issue entitled: Boosting structural food science published in Food Hydrocolloids.

* Corresponding author.

E-mail address: hans.bolinsson@ple.lth.se (H. Bolinsson).

¹ Hans Bolinsson and Martin Cramer Pedersen have contributed equally to the manuscript

<https://doi.org/10.1016/j.foodhyd.2025.111377>

Received 20 December 2024; Received in revised form 14 February 2025; Accepted 23 March 2025

Available online 24 March 2025

0268-005X/© 2025 The Authors. Published by Elsevier Ltd. This is an open access article under the CC BY license (<http://creativecommons.org/licenses/by/4.0/>).

Asymmetrical Flow Field-Flow Fractionation (AF4) presents a powerful experimental approach. The online coupling of AF4 to synchrotron SAXS on biomolecules has recently been demonstrated (Bolinsson et al., 2023; Börjesdotter et al., 2025; Graewert et al., 2023). SAXS is a widely used technique that provides information on the overall size, shape, and internal structure of colloidal particles like casein micelles at a nanometer resolution. It offers non-invasive probing of the internal packing of proteins and the spatial distribution of calcium phosphate clusters within the micelles, enabling detailed structural models to be built. Several such models have been proposed over the last 30 years (Bouchoux et al., 2010; Day et al., 2017; de Kruif et al., 2012; Ingham et al., 2016, 2018; Pedersen et al., 2022; Sorensen et al., 2013) providing increasingly refined ideas about the origin of the features in the scattering patterns. The most detailed modeling approach was presented recently providing a model that is consistent with current molecular knowledge of the casein components (Pedersen et al., 2022). However, SAXS alone cannot resolve the polydispersity or size heterogeneity of casein micelles in a bulk sample, a limitation that can be addressed by the combination with AF4.

AF4 is a versatile separation technique that allows fractionation of macromolecules and colloidal particles based on their hydrodynamic size without requiring a stationary phase (Wahlund & Giddings, 1987; Wahlund & Nilsson, 2012). In comparison to size-exclusion chromatography (SEC), the absence of a stationary phase in AF4 enables separation and resolution in a wider size-range, limits shearing of sample components, and minimizes interaction with the separation device as the surface area is several orders of magnitude smaller (Ramm et al., 2022). AF4 with light scattering detection has previously been applied for the separation and characterization of casein micelles in milk (Glantz et al., 2010; Lazzaro et al., 2017; Lie-Piang et al., 2021a, Lie-Piang et al., 2021a), enzymatically cross-linked casein aggregates (Abbate et al., 2019), and β -casein micelles (Cragnell et al., 2017). By coupling AF4 with SAXS (Bolinsson et al., 2023), it becomes possible to isolate populations of casein micelles with narrow size distributions and examine their structural properties in greater detail. This integrated approach allows for the analysis of micelle populations across a range of sizes, providing a more comprehensive understanding of the heterogeneity and structural organization of casein micelles in milk under different conditions.

At synchrotron facilities, the high flux and tunable energy of X-rays allow for rapid collection of high-quality SAXS data, enabling the study of complex biological systems such as casein micelles in detail. However, the vast amounts of data generated during such measurements, often collected at high throughput, present a significant challenge for manual data processing and analysis. An automated approach to data analysis becomes crucial in this context to handle the large datasets efficiently and to ensure consistency and accuracy in extracting meaningful structural parameters. Automated pipelines can already streamline processes such as background subtraction, normalization, radial averaging, and Guinier analysis (Konarev et al., 2003; Manalastas-Cantos et al., 2021; Panjkovich & Svergun, 2018), allowing researchers to quickly process and visualize data in real-time. Ultimately, automation ensures that the full potential of synchrotron SAXS data is realized, especially when combined with techniques like AF4, where the analysis must account for size-dependent variations across different micelle populations.

In this study, we present a new data analysis pipeline for AF4-SAXS data handling using the McSAS (Bressler et al., 2015) software to perform an automated data fitting routine based on pre-defined structural models, facilitating a more rapid interpretation of the hierarchical organization of casein micelles. This is performed by feeding the McSAS pipeline with hundreds of background-subtracted SAXS scattering curves extracted from AF4-SAXS fractograms. This allows for screening of AF4-SAXS fractograms for trends and specifics in size, shape and structural parameters.

2. Materials and methods

2.1. Sample and carrier liquid preparation

The AF4 carrier liquid of 50 mM Tris-(Hydroxymethyl)-amino-methane hydrochloride (Tris-HCl) and 2 mM CaCl_2 at pH 6.7, was prepared using Milli-Q water (Merck Millipore, Darmstadt, Germany). 0.02 % w/w NaN_3 was added to prevent bacterial growth. The analytical grade chemicals for preparation of carrier liquid were purchased from Merck KGaA, Darmstadt, Germany.

The skimmed milk sample was purchased in the grocery store and produced by Skånemejerier (Sweden) under the brand name Minimjölök. The skimmed milk was at the time of the purchase a homogenized, pasteurized (75–77 °C for 15 s) product containing 0.1 % w/w fat.

The milk was diluted x50 in the AF4 carrier liquid directly from the package stored under cold conditions at 6–8 °C, without any other treatment, and just prior to injection in the AF4.

2.2. CoSAXS beamline, MAX IV laboratory

The CoSAXS beamline at MAX IV has been constructed to deliver a high X-ray flux, 10^{13} photons/s at 12.4 keV, and a nominal wavelength of $\lambda = 0.99 \text{ \AA}$. The data was collected on an Eiger2 4 M (Dectris) detector within an evacuated flight tube, positioned at 8 m from the sample position. The detector at this position covers a q -range of $1.31 \times 10^{-3} < q < 0.15 \text{ \AA}^{-1}$, where $q = 4\pi\sin(\theta)/\lambda$, with 2θ the scattering angle and λ the X-ray wavelength. The flow cell consists of a 1 mm inner-diameter quartz capillary, with a 10 μm wall thickness. The acquisition rate during AF4-UV-SAXS fractionation was set to 1 frame/s.

2.3. AF4

The fractionation of milk was performed on an Eclipse 3+ AF4 system (Wyatt Technology, Dernbach, Germany). The carrier liquid flow to the channel was delivered by an isocratic pump, the samples were injected by an autosampler, and the channel was connected to a UV detector at 280 nm, all of which were from the 1100-series from Agilent, Santa Clara, USA. The UV detector outlet was connected directly to the sample flow-through quartz capillary of the synchrotron source using a 0.8 m long, 250 μm inner diameter, PEEK capillary. The software ASTRA (version 6.1.7.17, Wyatt Technology) was used for the acquisition of UV data. Data was also collected, on a separate occasion using multi angle light scattering (MALS), on an AF4-UV-MALS setup where the instrument configuration was the same except for the SAXS to MALS exchange. The MALS utilized was a Dawn Heleos II from Wyatt Technology, Santa Barbara, USA.

The carrier liquid was degassed by an in-line degasser and filtered before entering the channel and sample route by an in-line filter of mixed cellulose esters (MCE) with pore size 0.22 μm (Merck Millipore, Germany).

A short channel (SC) from Wyatt Technology was used for the fractionation. The channel height and area were defined by a 250 μm thick, wide mylar spacer (250W), with a tip-to-tip length of 174 mm. The membrane supporting frit was made from stainless steel. The ultrafiltration membrane acting as an accumulation wall during fractionation was a regenerated cellulose (RC) membrane from Nadir GmbH, Germany, with a molecular weight cutoff of 10 kDa.

The diluted milk sample was injected at 100 μl , corresponding to approximately 70 μg of injected protein mass. In the AF4 fractionation method the detector flow was set to 0.5 ml/min, focus flow to 3.3 ml/min, and injection flow to 0.2 ml/min. Injection was performed in focus mode for 3 min followed by focusing/relaxation for 3 min. The elution constituted three steps, starting with a constant cross flow of 3.3 ml/min for 5 min to fractionate the serum (whey) proteins and non-micellar caseins, followed by an exponentially decaying cross flow with a 2 min half-time until reaching a constant cross flow of 0.15 ml/min for 20

min.

2.4. Data processing

The initial data processing was done using Chromixs (Panjkovich & Svergun, 2018), with which a scattergram was produced for each of the data series, i.e. the total scattering intensity across each of the frames in the AF4-SAXS data series. An example of such a scattergram is shown in Fig. 1(a). From these scattergrams, sets of suitable frames representing the experimental background measurements were identified, averaged and used for subsequent background subtraction of all frames in the data series. Examples of such data sets are shown in Fig. 1(b) and (c). From this pipeline, a series of background subtracted SAXS profiles were obtained, as shown in Fig. 1(d), plotted as the scattering intensity, I , versus the scattering momentum transfer, q .

2.5. Data analysis - bayesian indirect fourier transform

The first element in the analysis pipeline was Indirect Fourier Transformation of the data (Glatter, 1977), with which pair distance distributions, $p(r)$, were produced, which informs about the overall geometry and compactness of the colloids in the sample. Specifically, the Bayesian version (BIFT) of this algorithm (Hansen, 2012a, 2012b; Larsen & Pedersen, 2021) was deployed. For each of the frames in the data series, the aforementioned $p(r)$ distributions were obtained, which are histograms of the pairwise distances, r , between the scatterers in the

colloidal particles (weighted by their contrast). From these the (scattering) radius of gyration, R_g , as well as the largest dimension, usually dubbed D_{max} , of the particles in the sample were inferred.

An example of a $p(r)$ distribution and the associated parameters is shown in Fig. 1(e). We plot these parameters across the data sets recorded near the principal peak in the scattergrams and AF4-UV signal in Fig. 3.

2.6. Data analysis - McSAS

The SAXS data analysis continued by subjecting each of the frames to the McSAS analysis tool (Bressler et al., 2015). The tool was set up to refine a hypothetical distribution of spherical particles, which adequately accounts for the shape of each of the scattering profiles in the data. This output was presented as histograms of sphere radii, R . An example of this analysis process is shown in Fig. 1(f). These distributions of radii were then binned into three separate categories based on the general understanding of casein micelle structure, i.e. below 10 nm, between 10 and 40 nm, and above 40 nm, capturing sub-micellar structure, micellar structure, and superstructures respectively, and the evolution of these were monitored across the same data sets as for the Indirect Fourier Transformation analysis. This information is displayed in Fig. 4.

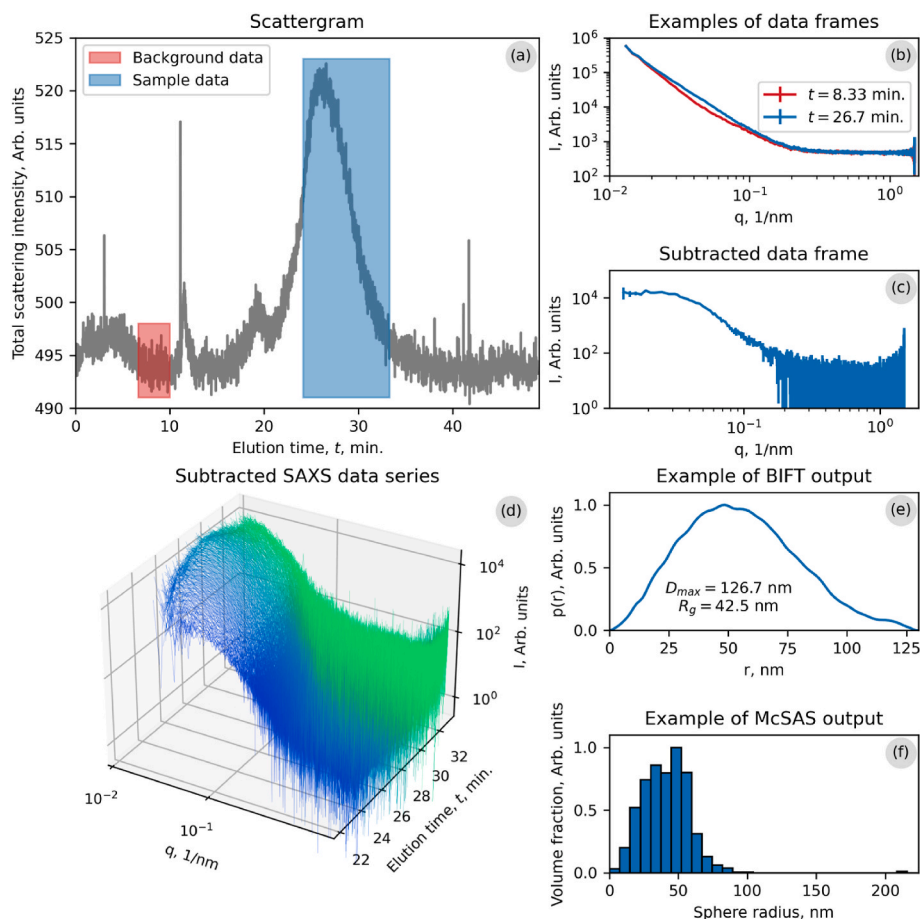


Fig. 1. Overview of the data processing pipeline. Following the AF4-SAXS experiment, the total scattering intensity in each recorded data frame was plotted to ascertain which frames to treat as background and sample frames (as shown in (a)). In (b) and (c), examples of such data frames are shown. All data frames were subjected to background subtraction to obtain the data series shown in (d). Each of these data sets were then analyzed using the Bayesian Indirect Fourier Transformation (BIFT) and the McSAS algorithms, from which $p(r)$ distributions and a histogram capturing the output of the McSAS analysis were obtained. Examples of these are shown in (e), where r represents distances between scattering pairs, and (f).

3. Results and discussion

Fig. 2 shows the cumulative and differential weight fractions of casein micelles in the milk sample, extracted from AF4-UV-RI-MALS measurement. Utilizing MALS allows for characterization of the size range of interest for this study. MALS results were obtained by applying the Berry model for angular dependency fitting. The dn/dc value used for the evaluation was 0.185 ml/g, which is of general use for protein assemblies. The main portion of the casein micelles are found in the R_g -range of 35–100 nm. Less than 10 % of the micelles show sizes in the range 100–150 nm. The most abundant size of casein micelles appears in the size range 45–50 nm. It should be mentioned that the fractogram of milk in Fig. 2 a) was collected under different flow conditions compared to conditions used for AF4-UV-SAXS measurements.

Fig. 3 shows the overlaid UV and SAXS fractograms from AF4-UV-SAXS of the milk sample. The fraction eluting at 10–12 min corresponds to serum proteins and albumins; the fraction eluting at approximately 20 min corresponds to non-micellar caseins and aggregates/oligomers thereof; the main peak eluting at 22–35 min corresponds to protein, i.e. casein micelles. The casein micelle peak has previously been shown to contain no co-eluting species (Glantz et al., 2010). The SAXS data was adequate for further analysis in the elution time range 24–33 min, indicated by blue vertical lines in Fig. 3. The scattering signal from serum proteins, non-micellar and aggregated caseins was insufficient for further analyses.

Fig. 4 shows the results from the McSAS/BIFT pipeline presented above. The largest dimension, D_{max} , and the radius of gyration, R_g , are plotted as functions of elution time, Fig. 4(a) and (b). AF4 fractionates according to increasing hydrodynamic size. As expected R_g and D_{max} show increasing values over the casein micelles peak in the elution time range 24–33 min.

The BIFT ratio, Fig. 4(c), shows the $2R_g/D_{max}$ ratio. The R_g/R_h ratio is commonly used for extracting shape information from light scattering experiments (Burchard, 1999; Nilsson, 2013). Here we consider the BIFT ratio as an equivalent, meaning that D_{max} is approximated by $2R_h$. This approximation should hold for hard spheres, spherical particles with a homogeneous density and consequently smooth surface. Since casein micelles are considered covered by a hairy layer of κ -casein (Holt & Horne, 1996), a thereby induced deviation is expected. Internal cavities create a density inhomogeneity which also results in deviation from a hard sphere. The R_g/R_h ratio for a spherical entity with homogeneous mass distribution is $\sqrt{3/5}$, i.e. approximately 0.77. The $2R_g/D_{max}$ for casein micelles are here showing values of 0.7–0.8, which is near what is expected for spherical particles.

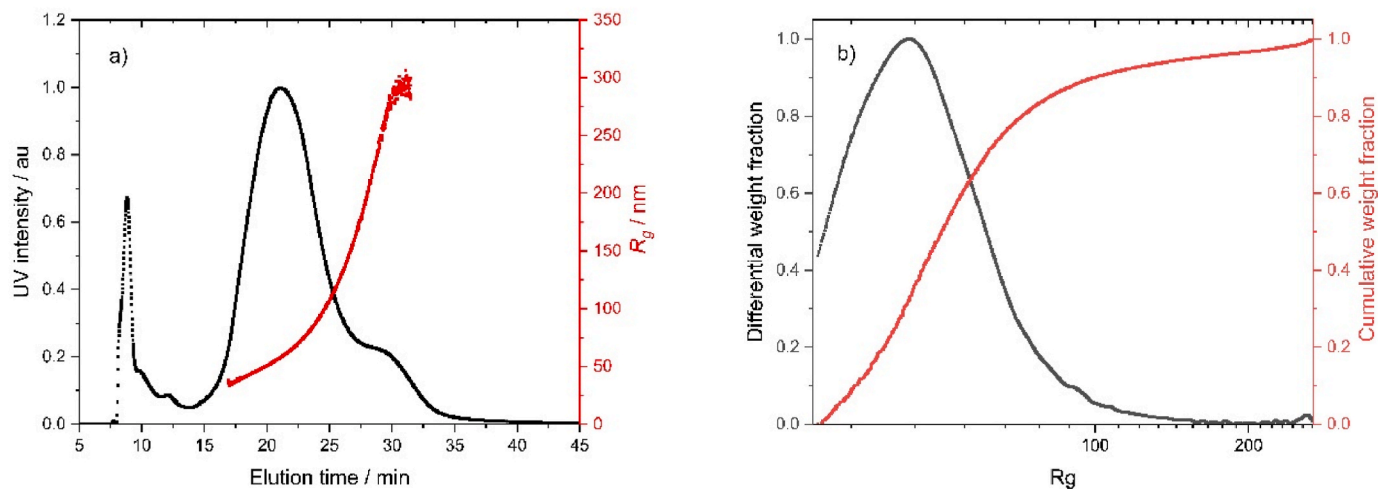


Fig. 2. a) UV fractogram of milk with R_g -distribution in red, b) Cumulative and differential weight fractions of casein micelles in the milk sample. 90 % of the casein micelles appear in the size range 35–100 nm. The most abundant size of casein micelles is in the size range 45–50 nm.

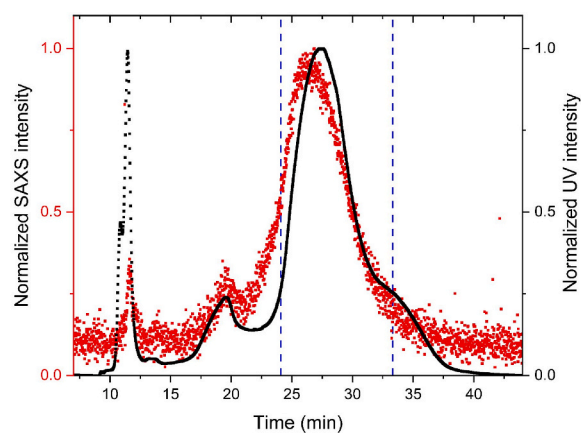


Fig. 3. AF4-UV-SAXS fractogram showing normalized UV (black) and SAXS (red) intensities vs elution time for milk. Blue lines indicate the range of SAXS data used for McSAS/BIFT pipeline evaluation.

From the McSAS analysis, Fig. 4(d), the contribution to the total scattering from each of the predefined length scales is visualized as a function of elution time. Length scales below 10 nm are intended to catch contributions to the scattering from colloidal calcium phosphate particles (CCPs), and possibly also protein heterogeneities/particles (PP) (Pedersen et al., 2022). The CCPs are found in the size range 2–4 nm (Horne, 2020; Pedersen et al., 2022; Trejo et al., 2011). The intermediate length scale range, 10–40 nm, intends to catch incompressible regions and/or internal cavities (Hettiarachchi et al., 2020; Pedersen et al., 2022; Trejo et al., 2011). The SAXS scattering from the smallest micelles, eluting before minute 24, were not included in the pipeline analysis due to insufficient signal-to-noise (S/N) or possibly impaired signal due to co-elution of fractions. The length scale $R > 40$ nm can therefore safely be said to cover scattering contributions from the overall size of micelles, except for the micelles eluting early, before minute 26. However, a micelle of size $R \approx 40$ nm can hardly contain internal cavities of size 20–40 nm and still be considered a micelle.

It should be stressed that the sample is not believed to be composed of simple polydisperse spherical particles in solution (Glantz et al., 2010) and that this analysis method was merely deployed to highlight the changes in the relevant length-scales of the sample throughout the elution period. In other words, while a model of polydisperse spherical particles is certainly an oversimplification of the complex geometry of

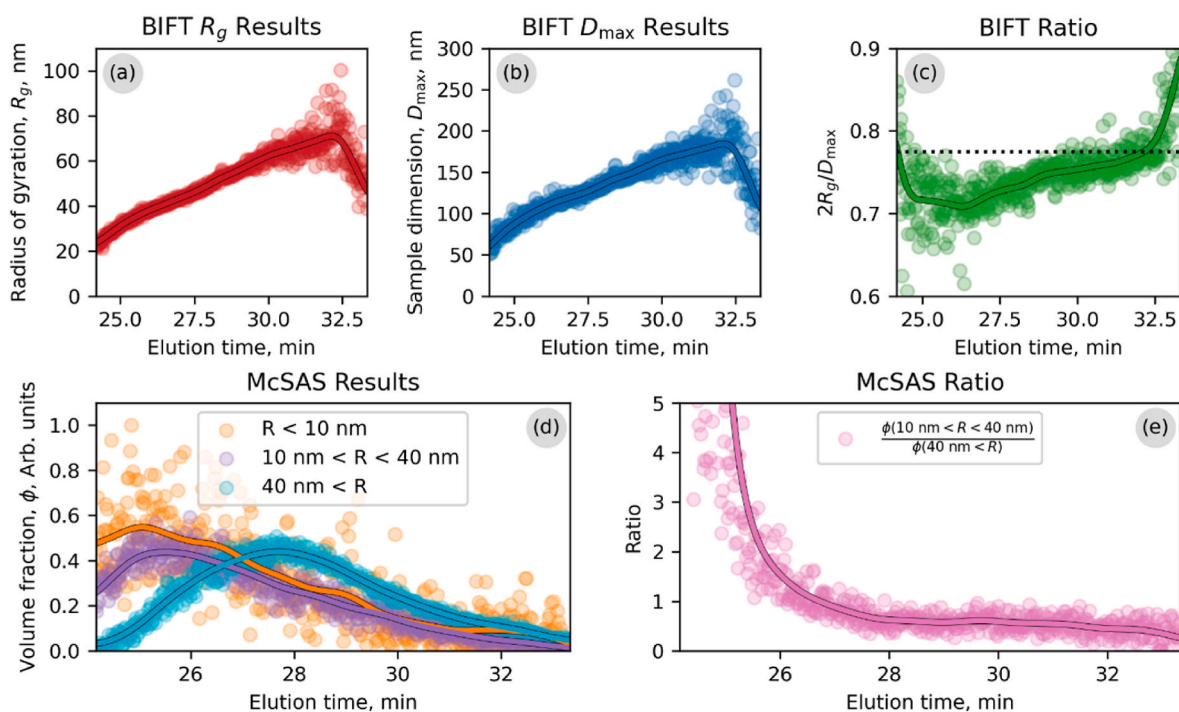


Fig. 4. Results from McSAS/BIFT analysis pipeline. (a) and (b) visualize the main outputs from the BIFT analysis. (c) presents the BIFT ratio for, assessment of compactness of our sample, and comparison to the value corresponding to a homogeneous sphere (dashed line). In (d), the McSAS results are binned in specific size ranges matching length scales (R) of particular interest. In (e), the ratio of two length scales was computed to ascertain the degree to which the intermediate range signal precedes the larger. In all plots, rolling averages of the computed quantities are shown (full lines).

casein micelles, it does allow analysis and quantification of scattering data in a systematic and somewhat unbiased fashion.

The flexibility of the McSAS framework is extensive. These analyses could be carried out using different modeling assumptions; basing the refinement on e.g. prolate or oblate ellipsoidal particles or other geometric shapes for which the scattering contribution is readily calculated. In turn, such analysis schemes would yield more distributions of model parameters, and it could be interesting to compare the outcomes of different analysis schemes in order to highlight subtle differences across the elution series.

The volume fraction contribution to the total scattering from length scales $R < 10$ nm shows a negative slope over the elution time range, i.e. as a function of increasing hydrodynamic size. Most interestingly, this contribution peaks at 25–26 min, where the smallest micelles elute. This is indicative of a difference in micelle composition over the size range, with smaller micelles possibly exhibiting a higher concentration of CCP/PP. In Fig. 3 it can be observed that the casein micelles peak position differs between SAXS and UV signal. This is possibly also a result of decreasing electron density as a function of increasing micelle size.

For the intermediate sizes, $10 < R < 40$ nm, a relative volume fraction in relation to sizes $R > 40$ nm was performed, Fig. 4(e). The relative volume fraction of internal cavities with micelle size is approximately constant for elution times >27.5 min, indicating a consistent micelle build-up. The peak below 27.5 min can be attributed to a structural scattering contribution from a combination of micelle sizes and internal cavities. They are not distinguishable in that size range, with only the method used here.

For the length scale $R < 10$ nm the relative volume fraction analysis could in principle have been performed, but for adequate results, a higher resolution and S/N is needed. To achieve a higher S/N a higher sample load and lower dilution of the sample in the AF4 channel is mandatory. Higher concentration in fractions eluting from the AF4 channel can either be achieved by increasing the sample mass loading in the channel or by decreasing the dilution of the sample zone as it exits the channel. Increasing the sample mass loading will eventually lead to

overloading effects, i.e. inadequate sample relaxation, and impaired fractionation (van Bruijnsvoort et al., 2001). To some extent, this can be compensated for by using frit-inlet injection which has been shown to allow for a substantial increase in mass load as previously demonstrated for ultra-large biopolymers (Fuentes et al., 2019). To decrease sample dilution, splitting the outlet stream from the channel just before the sample zone exits the channel is likely to be an efficient approach (Wahlund et al., 1986). This way a large part of the sample depleted stream above the sample zone can be removed prior to entering the detectors.

The large length scale, $R > 40$ nm, shows a peak at 27–28 min. The contribution to the scattering profile follows the UV fractogram in Fig. 3 and is reflecting a combination of volume fraction and overall micelle size.

4. Conclusion

The vast amounts of data generated during an AF4-UV-SAXS measurement, collected at high throughput, present a significant challenge for manual data processing and analysis. An automated approach to data analysis becomes crucial in this context to handle the large datasets efficiently and to ensure consistency and accuracy in extracting meaningful structural parameters. In this study we have presented a way of performing automated analysis on hundreds of scattering curves from an AF4 size fractionated milk sample. The results show that this methodology can be used to extract differences and trends in typical SAXS parameters like shape, structure and size over an eluted size range. The methodology combines existing evaluation tools for AF4-SAXS with automation in a pipeline redefined to handle analysis of SAXS scattering curves in an automated way. The use of AF4 for size fractionation of the sample prior to on-line SAXS acquisition, enables shape and structural analysis of individual and isolated hydrodynamic sizes within the sample. On top of that AF4 also separates out every constituent of the sample which is not represented in the size range of casein micelles. Consider a batch measurement of milk, where serum proteins, caseins of various

kinds and aggregates/oligomers thereof, and the micelles, which would be measured as a sum-weighted scattering from all different constituents.

AF4 as a separation method excels when it comes to fractionation of widely size-distributed samples of complex nature, like the casein micelles in milk. In comparison to other separation techniques, the low shear forces and interactive surface area in the separation device makes it the first choice for sensitive samples. With SEC, which is frequently used in SEC-SAXS setups, it would not be possible to fractionate a milk sample without perturbing the integrity of individual micelles due to the high shear forces induced.

The results presented in this study represent initial trials for casein micelle characterization utilizing AF4-UV-SAXS. The next step will be to improve data quality, which primarily encompasses increasing the concentration in fractions eluting from the AF4 channel, giving an increase in S/N in the SAXS data. Recent results using a different AF4 setup have shown a considerable increase in fraction concentrations when performing on-line AF4-SAXS for the characterization of lipid nanoparticles and this approach should now be adapted for studying casein micelles in milk. This approach has the potential to enhance the precision and depth of casein micelle analysis, enabling more detailed insights into their structure and dynamic behavior. An interesting study for the future would be to study the progress of the same graphs for milk equilibrated at different times in a set of temperatures. The dynamics of bovine casein micelles have been studied before and it has been shown that the solubility of β -casein and calcium decreases with increasing temperature (Liu et al., 2013). The method used here could give insights in the progress of casein micelle dynamics and add an extra piece to the puzzle of entangling the casein micelle hierarchical structure.

CRedit authorship contribution statement

Hans Bolinsson: Writing – review & editing, Writing – original draft, Visualization, Validation, Resources, Project administration, Methodology, Investigation, Formal analysis, Data curation, Conceptualization. **Martin Cramer Pedersen:** Writing – review & editing, Writing – original draft, Visualization, Validation, Software, Methodology, Investigation, Formal analysis, Data curation, Conceptualization. **Maria Glantz:** Writing – review & editing, Investigation, Formal analysis. **Fátima Herranz-Trillo:** Writing – review & editing, Resources, Methodology, Investigation, Data curation. **Jacob Judas Kain Kirkensgaard:** Writing – review & editing, Writing – original draft, Visualization, Validation, Methodology, Investigation, Formal analysis, Data curation, Conceptualization. **Lars Nilsson:** Writing – review & editing, Writing – original draft, Visualization, Validation, Supervision, Resources, Project administration, Methodology, Investigation, Funding acquisition, Formal analysis, Conceptualization.

Funding

This research is a part of NextBioForm, an industrial consortium supported by the Swedish Governmental Agency for Innovation System (VINNOVA, ref 2018–04730).

Declaration of competing interest

The authors declare that they have no known competing financial interests or personal relationships that could have appeared to influence the work reported in this paper.

Acknowledgements

We would like to thank MAX IV Laboratory for beamtime on Beamline CoSAXS under Proposal 20220489. Research conducted at MAX IV, a Swedish national user facility, is supported by the Swedish Research council under contract 2018–07152, the Swedish

Governmental Agency for Innovation Systems under contract 2018–04969, and Formas under contract 2019–02496.

Data availability

Data will be made available on request.

References

- Abbate, R. A., Raak, N., Boye, S., Janke, A., Rohm, H., Jaros, D., & Lederer, A. (2019). Asymmetric flow field flow fractionation for the investigation of caseins cross-linked by microbial transglutaminase. *Food Hydrocolloids*, 92, 117–124. <https://doi.org/10.1016/j.foodhyd.2019.01.043>
- Bolinsson, H., Söderberg, C., Herranz-Trillo, F., Wahlgren, M., & Nilsson, L. (2023). Realizing the AF4-UV-SAXS on-line coupling on protein and antibodies using high flux synchrotron radiation at the CoSAXS beamline, MAX IV. *Analytical and Bioanalytical Chemistry*, 415(25), 6237–6246. <https://doi.org/10.1007/s00216-023-04900-7>
- Börjesdotter, A. M., Bolinsson, H., Dagö, T., Herranz-Trillo, F., Palmiero, U. C., Schagerlöf, H., & Nilsson, L. (2025). Lipid nanoparticle properties explored using online asymmetric flow field-flow fractionation coupled with small angle X-ray scattering: Beyond average characterisation. *International Journal of Pharmacy*, 668, Article 124940. <https://doi.org/10.1016/j.ijpharm.2024.124940>
- Bouchoux, A., Gesan-Guiziou, G., Perez, J., & Cabane, B. (2010). How to squeeze a sponge casein micelles under osmotic stress, a SAXS study. *Biophysical Journal*, 99(11), 3754–3762. <https://doi.org/10.1016/j.bpj.2010.10.019>
- Bressler, I., Pauw, B. R., & Thünemann, A. F. (2015). McSAS: Software for the retrieval of model parameter distributions from scattering patterns. *Journal of Applied Crystallography*, 48, 962–969. <https://doi.org/10.1107/S1600576715007347>
- Burchard, W. (1999). Solution properties of branched macromolecules. *Advances in Polymer Science*, 143, 113–194.
- Cragnell, C., Choi, J., Segad, M., Lee, S., Nilsson, L., & Skepö, M. (2017). Bovine β -casein has a polydisperse distribution of equilibrium micelles. *Food Hydrocolloids*, 70, 65–68. <https://doi.org/10.1016/j.foodhyd.2017.03.021>
- Dalgleish, D. G. (2011). On the structural models of bovine casein micelles—review and possible improvements [10.1039/C0SM00806K]. *Soft Matter*, 7(6), 2265–2272. <https://doi.org/10.1039/C0SM00806K>
- Dalgleish, D. G., & Corredig, M. (2012). The structure of the casein micelle of milk and its changes during processing. *Annual Review of Food Science and Technology*, 3, 449–467. <https://doi.org/10.1146/annurev-food-022811-101214>
- Day, L., Raynes, J. K., Leis, A., Liu, L. H., & Williams, R. P. W. (2017). Probing the internal and external micelle structures of differently sized casein micelles from individual cows milk by dynamic light and small-angle X-ray scattering. *Food Hydrocolloids*, 69, 150–163. <https://doi.org/10.1016/j.foodhyd.2017.01.007>
- de Kruif, C. G., Huppertz, T., Urban, V. S., & Petukhov, A. V. (2012). Casein micelles and their internal structure. *Advances in Colloid and Interface Science*, 171, 36–52. <https://doi.org/10.1016/j.cis.2012.01.002>
- Fuentes, C., Choi, J., Zielke, C., Peñarrieta, J. M., Lee, S., & Nilsson, L. (2019). Comparison between conventional and frit-inlet channels in separation of biopolymers by asymmetric flow field-flow fractionation. *Analyst*, 144(15), 4559–4568. <https://doi.org/10.1039/c9an00466a>
- Glantz, M., Håkansson, A., Månsson, H. L., Paulsson, M., & Nilsson, L. (2010). Revealing the size, conformation, and shape of casein micelles and aggregates with asymmetrical flow field-flow fractionation and multiangle light scattering. *Langmuir*, 26(15), 12585–12591. <https://doi.org/10.1021/la101892x>
- Glatter, O. (1977). Data evaluation in small-angle scattering - calculation of radial electron-density distribution by means of indirect Fourier transformation. *Acta Physica Austriaca*, 47(1–2), 83–102. <Go to ISI>://WOS:A1977DP80000004.
- Graewert, M. A., Wilhelmy, C., Bacic, T., Schumacher, J., Blanchet, C., Meier, F., Drexel, R., Welz, R., Kolb, B., Bartels, K., Nawroth, T., Klein, T., Svergun, D., Langguth, P., & Haas, H. (2023). Quantitative size-resolved characterization of mRNA nanoparticles by in-line coupling of asymmetrical-flow field-flow fractionation with small angle X-ray scattering. *Scientific Reports*, 13(1), Article 15764. <https://doi.org/10.1038/s41598-023-42274-z>
- Hansen, S. (2012a). BayesApp: A web site for indirect transformation of small-angle scattering data. *Journal of Applied Crystallography*, 45, 566–567. <https://doi.org/10.1107/s0021889812014318>
- Hansen, S. (2012b). Bayesian methods in SAXS and SANS structure determination. In T. Hamelryck, K. Mardia, & J. Ferkinghoff-Borg (Eds.), *Bayesian methods in structural bioinformatics* (pp. 313–342). Springer Berlin Heidelberg. https://doi.org/10.1007/978-3-642-27225-7_13
- Hettiarachchi, C. A., Swilius, M. T., & Harte, F. M. (2020). Assessing constituent volumes and morphology of bovine casein micelles using cryo-electron tomography. *Journal of Dairy Science*, 103(5), 3971–3979. <https://doi.org/10.3168/jds.2019-17016>
- Holt, C. (2022). Quantitative multivalent binding model of the structure, size distribution and composition of the casein micelles of cow milk. *International Dairy Journal*, 126, Article 105292. <https://doi.org/10.1016/j.idairyj.2021.105292>
- Holt, C., & Horne, D. (1996). The hairy casein micelle: Evolution of the concept and its implications for dairy processing. *Netherlands Milk and Dairy Journal*, 50, 1–27.
- Horne, D. S. (2020). Chapter 6 - casein micelle structure and stability. In M. Boland, & H. Singh (Eds.), *Milk proteins* (3rd ed., pp. 213–250). Academic Press. <https://doi.org/10.1016/B978-0-12-815251-5.00006-2>

- Ingham, B., Smialowska, A., Erlangga, G. D., Matia-Merino, L., Kirby, N. M., Wang, C., Haverkamp, R. G., & Carr, A. J. (2016). Revisiting the interpretation of casein micelle SAXS data [10.1039/C6SM01091A]. *Soft Matter*, 12(33), 6937–6953. <https://doi.org/10.1039/C6SM01091A>
- Ingham, B., Smialowska, A., Kirby, N. M., Wang, C., & Carr, A. J. (2018). A structural comparison of casein micelles in cow, goat and sheep milk using X-ray scattering [10.1039/C8SM00458G]. *Soft Matter*, 14(17), 3336–3343. <https://doi.org/10.1039/C8SM00458G>
- Konarev, P. V., Volkov, V. V., Sokolova, A. V., Koch, M. H. J., & Svergun, D. I. (2003). Primus: A windows PC-based system for small-angle scattering data analysis. *Journal of Applied Crystallography*, 36, 1277–1282. <https://doi.org/10.1107/s0021889803012779>
- Larsen, A. H., & Pedersen, M. C. (2021). Experimental noise in small-angle scattering can be assessed using the Bayesian indirect Fourier transformation. *Journal of Applied Crystallography*, 54(5), 1281–1289. <https://doi.org/10.1107/S1600576721006877>
- Lazzaro, F., Saint-Jalmes, A., Violleau, F., Lopez, C., Gaucher-Delmas, M., Madec, M.-N., Beaucher, E., & Gaucheron, F. (2017). Gradual disaggregation of the casein micelle improves its emulsifying capacity and decreases the stability of dairy emulsions. *Food Hydrocolloids*, 63, 189–200. <https://doi.org/10.1016/j.foodhyd.2016.08.037>
- Lie-Piang, A., Leeman, M., Castro, A., Börjesson, E., & Nilsson, L. (2021a). Investigating the effect of powder manufacturing and reconstitution on casein micelles using asymmetric flow field-flow fractionation (AF4) and transmission electron microscopy. *Food Research International*, 139. <https://doi.org/10.1016/j.foodres.2020.109939>. Article 109939.
- Lie-Piang, A., Leeman, M., Castro, A., Börjesson, E., & Nilsson, L. (2021b). Revisiting the dynamics of proteins during milk powder hydration using asymmetric flow field-flow fractionation (AF4). *Current Research in Food Science*, 4, 83–92. <https://doi.org/10.1016/j.crfs.2021.02.004>
- Liu, D. Z., Weeks, M. G., Dunstan, D. E., & Martin, G. J. O. (2013). Temperature-dependent dynamics of bovine casein micelles in the range 10–40°C. *Food Chemistry*, 141(4), 4081–4086. <https://doi.org/10.1016/j.foodchem.2013.06.130>
- Manalastas-Cantos, K., Konarev, P. V., Hajizadeh, N. R., Kikhney, A. G., Petoukhov, M. V., Molodenskiy, D. S., Panjkovich, A., Mertens, H. D. T., Gruzinov, A., Borges, C., Jeffries, C. M., Svergun, D. I., & Franke, D. (2021). Atsas 3.0: Expanded functionality and new tools for small-angle scattering data analysis. *Journal of Applied Crystallography*, 54, 343–355. <https://doi.org/10.1107/s1600576720013412>
- Nilsson, L. (2013). Separation and characterization of food macromolecules using field-flow fractionation: A review. *Food Hydrocolloids*, 30(1), 1–11. <https://doi.org/10.1016/j.foodhyd.2012.04.007>
- Panjkevich, A., & Svergun, D. I. (2018). Chromixs: Automatic and interactive analysis of chromatography-coupled small-angle X-ray scattering data. *Bioinformatics*, 34(11), 1944–1946. <https://doi.org/10.1093/bioinformatics/btx846>
- Pedersen, J. S., Moller, T. L., Raak, N., & Corredig, M. (2022). A model on an absolute scale for the small-angle X-ray scattering from bovine casein micelles. *Soft Matter*, 18(45), 8613–8625. <https://doi.org/10.1039/d2sm00724j>
- Ramm, I., Leeman, M., Schagerlöf, H., León, I. R., Castro, A., & Nilsson, L. (2022). Investigation of native and aggregated therapeutic proteins in human plasma with asymmetrical flow field-flow fractionation and mass spectrometry. *Analytical and Bioanalytical Chemistry*, 414(29), 8191–8200. <https://doi.org/10.1007/s00216-022-04355-2>
- Sorensen, H., Pedersen, J. S., Mortensen, K., & Ipsen, R. (2013). Characterisation of fractionated skim milk with small-angle X-ray scattering. *International Dairy Journal*, 33(1), 1–9. <https://doi.org/10.1016/j.idairyj.2013.05.006>
- Trejo, R., Dokland, T., Jurat-Fuentes, J., & Harte, F. (2011). Cryo-transmission electron tomography of native casein micelles from bovine milk. *Journal of Dairy Science*, 94(12), 5770–5775. <https://doi.org/10.3168/jds.2011-4368>
- Tuinier, R., & de Kruijff, C. G. (2002). Stability of casein micelles in milk. *The Journal of Chemical Physics*, 117(3), 1290–1295. <https://doi.org/10.1063/1.1484379>
- van Bruijnsvoort, M., Wahlund, K. G., Nilsson, G., & Kok, W. T. (2001). Retention behaviour of amylopectins in asymmetrical flow field-flow fractionation studied by multi-angle light scattering detection. *Journal of Chromatography A*, 925(1–2), 171–182. [https://doi.org/10.1016/s0021-9673\(01\)01020-2](https://doi.org/10.1016/s0021-9673(01)01020-2)
- Wahlund, K. G., & Giddings, J. C. (1987). Properties of an asymmetrical flow field-flow fractionation channel having one permeable wall. *Analytical Chemistry*, 59(9), 1332–1339. <https://doi.org/10.1021/ac00136a016>
- Wahlund, K.-G., & Nilsson, L. (2012). Flow FFF – basics and key applications. In S. K. R. Williams, & K. D. Caldwell (Eds.), *Field-flow fractionation in biopolymer analysis* (pp. 1–21). Vienna: Springer. https://doi.org/10.1007/978-3-7091-0154-4_1
- Wahlund, K. G., Winegarner, H. S., Caldwell, K. D., & Giddings, J. C. (1986). Improved flow field-flow fractionation system applied to water-soluble polymers: Programming, outlet stream splitting, and flow optimization. *Analytical Chemistry*, 58(3), 573–578. <https://doi.org/10.1021/ac00294a018>